FAN UNIT WITH COMPACT GUIDE VANE DESIGNED FOR LOW HUB RATIO AXIAL FANS

Walter ANGELIS, Frieder LÖRCHER

ZIEHL-ABEGG SE, Ventilation Division, Heinz-Ziehl-Strasse, 74653 Künzelsau, Germany

SUMMARY

In the present work, guide vane designs are investigated for axial fans with low hub-to-tip ratio. In these configurations, a detached flow region in the vicinity of the hub often occurs. The presence of this hub recirculation zone is shown to be the reason why classical guide vane designs in this case don't result in a significant increase of static efficiency. A RANS CFD model is calibrated in order to predict correctly the extension of the hub dead water. Using this model, a guide vane unit geometry showing a high static efficiency gain for axial fans with low hub-to-tip ratio is developed. For this unit, numerical and experimental results are presented.

INTRODUCTION

In the development of low pressure axial fans for refrigeration, air conditioning, ventilation, heating, energy regeneration, cleanroom technology, agricultural and similar applications, energetic efficiency today plays, besides noise level reduction, a key role. The reasons for that are growing energy costs and the need to reduce CO_2 emissions. Nevertheless, low pressure fans without guide vanes are still widely used, mainly due to the low production costs and the need for high axial packaging (axial compactness) of the fans. Low pressure axial fans typically have low hub-to-tip ratios $\nu = R_{Hub} / R_{Tip}$ of about 0.2-0.5. The reason for that is, on the one hand, that high volume flow rates are required at low pressure rise and, on the other hand, that the outer motor contour of external rotor motors is used as impeller hub. It is known from literature [5,6], that classical guide vane design, where the reduction of the circumferential flow component to near-zero values is intended, often leads to poor performance for fans with low hub ratio, meaning that there is no or only a small improvement in the static efficiency. This fact may be a further reason why guide vanes are rarely used for this class of fans. In the present work, an axially compact guide vane design is presented suitable to increase significantly the static efficiency of axial fans with low hub-to-tip ratio.

HUB DEAD WATER AND ITS IMPACT

Occurrence of hub dead water

It is known [1, 2, 3] that typically for fans with low hub-to-tip ratio $\nu < 0.5$, a phenomenon called hub dead water occurs, meaning the existence of a near-hub recirculating flow region not

contributing to the effective fluid transport from inlet to outlet. A simplified criterion mentioned for the onset of hub separation (see [3]) is the ratio of the circumferential to the axial velocity component downstream the fan v_θ / v_x, which should not fall below values of $0.8..1$ in order to avoid hub dead water. The cross-section, which is effectively available for fluid transport, is the mechanically available cross-section reduced by the cross-section of the hub dead water zone. In *Figure 1*, the presence of hub separation is illustrated by the visualization of meridional streamlines obtained by a CFD-simulation of a rotor-only axial fan with low hub ratio $\nu = 0.24$ at two different operation points. The fan rotor has a diameter of 630 mm. The blades of the fan are twisted and forward-swept, with a stacking angle at the tip of 30°. They have profiled cross-section, a serrated trailing edge and the blade tip geometry is formed as winglet. The hub contour is a simplified representation of the outer contour of the existing electrical fan motor. In particular, at the duty point with higher pressure rise with dimensionless volume flow $\varphi = 0.25$ and dimensionless static pressure rise $\psi_{stat} = 0.16$, the formation of a significant hub dead water region can be observed. The effective area used for the through-flow is obviously reduced by the recirculation region near the hub. In general, at duty points with higher pressure rise, the occurrence of hub dead water is more pronounced.

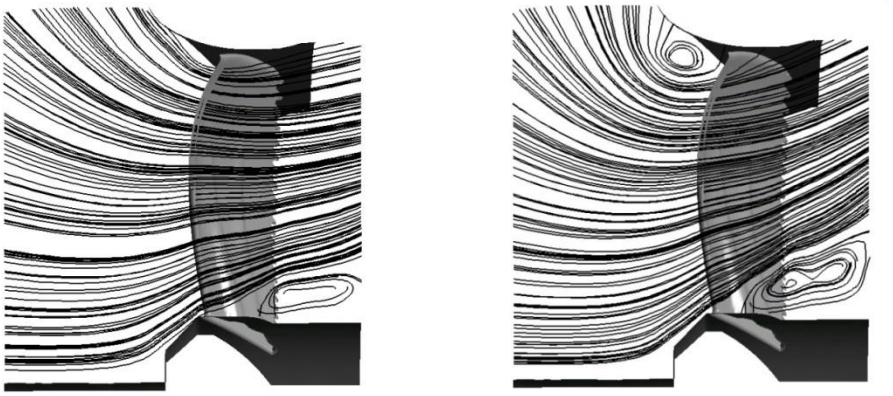

Figure 1: Meridional streamlines of a rotor-only axial fan (only, CFD results) at $\varphi = 0.3$ *and* $\psi_{stat} = 0.1$ *(left) and at* $\varphi = 0.25$ *and* $\psi_{stat} = 0.16$ *(right)*

Impact of detached flow in the hub region on static efficiency (without guide vane)

The existence of a hub separation zone is detrimental for static efficiency. Dynamic fluid energy at the fan outlet has to be considered as loss for many typical arrangements of low pressure axial fans. A typical, simplified partition of the shaft input energy to the airflow as derived from CFD results is depicted in *Figure 2*.

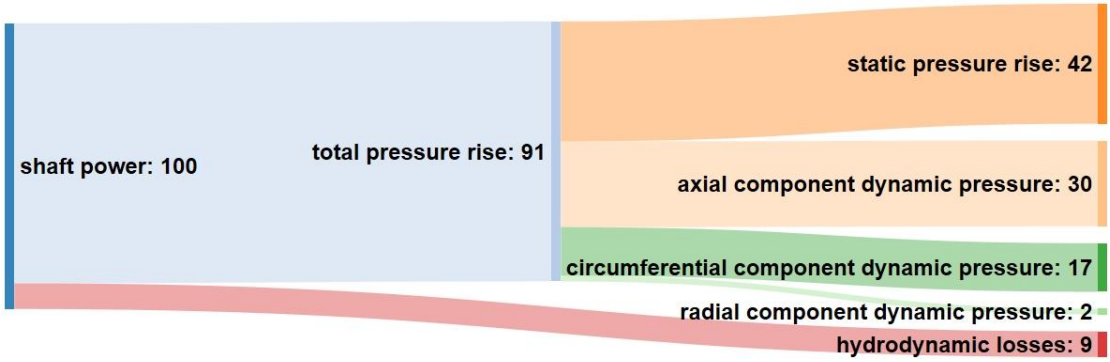

Figure 2: Typical partition of shaft power to different types of fluid energy for an axial fan without guide vane at $\varphi = 0.25$ *and* $\psi_{stat} = 0.16$*. All numbers in %.*

The only part of the shaft input power (100%) contributing to the static efficiency is the branch "static pressure rise". Thus in this case, the static efficiency is $\eta_{stat} = 42\,\%$. We note that the part of the circumferential velocity component, which is reacted to static pressure downstream of the fan (as described for example in [8, 9]), is already added to the part "static pressure rise". The biggest branches considered as loss are the dynamic pressures at the fan outlet constituted by axial and circumferential velocities. The weights vary depending on the operation point, for the graph we chose as operation point $\varphi = 0.25$ and $\psi_{stat} = 0.16$, having a volume flow rate slightly higher than the point of maximum static efficiency. By means of a guide vane, the circumferential component dynamic pressure could be theoretically reacted to static pressure. The contribution of the axial velocity component is mainly controlled by the mean axial velocity $v_{x,mean} = \dot{V} / A_{eff}$, where A_{eff} denotes the effectively by the main flow in x-direction engaged cross section area. In this consideration, the region occupied by the hub dead water does not contribute to A_{eff}. So, at given volume flow rate, the presence of hub dead water increases the dynamic pressure contribution of the axial velocity thus penalizing the static efficiency.

Conventional guide vane design in the presence of hub dead water

In this section, we present results from classical guide vane design, as described for example in [7, 9], applied to axial fans with low hub ratio and occurrence of hub dead water. We note that the mentioned authors restricted the design to higher hub-ratios (indeed, minimal hub-to-tip ratios, being significantly higher than the low hub ratios considered in this work, are given by the authors depending on operation points). A main characteristic of these guide vanes is that they are designed such that the circumferential velocity component is driven to near-zero values and reacted to static pressure. Therefore the trailing edge blade angles are nearby 0° or even negative. The following example shows, that such guide vane design leads, for the considered class of fans, to poor performance (in the sense that the static efficiency is not significantly improved compared to the rotor-only fan configuration).

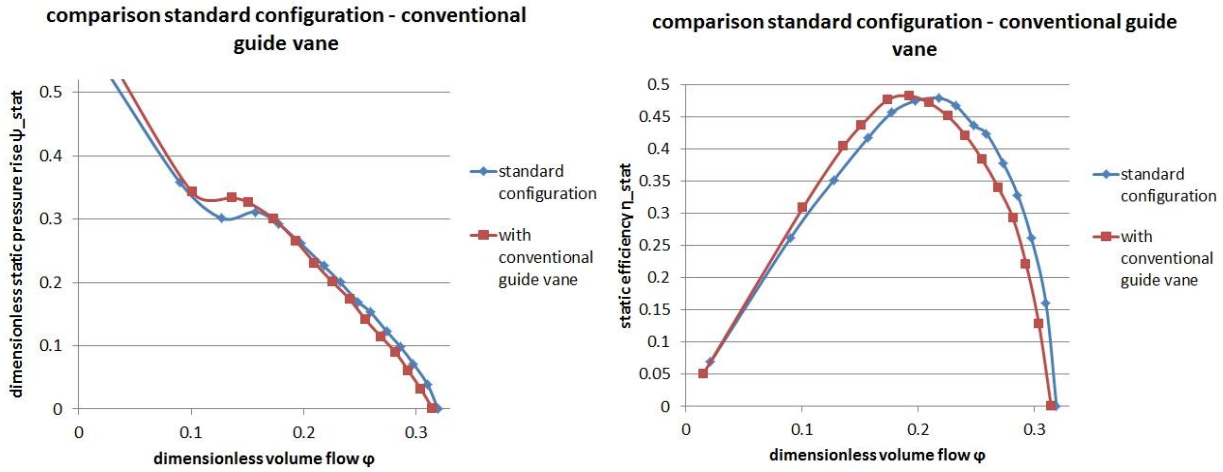

Figure 3: Experimental comparison of fan without guide vane and fan with conventional guide vane

In *Figure 3*, results of an experiment with conventional guide vane geometry are depicted. In an overall view, a significant improvement by the guide vane cannot be observed. Especially for duty points with higher volume flows, the static efficiency is even deteriorated. The reasons for this behavior have been investigated by 5-hole-probe experiments and CFD simulations at the volume flow rate $\varphi = 0.25$.

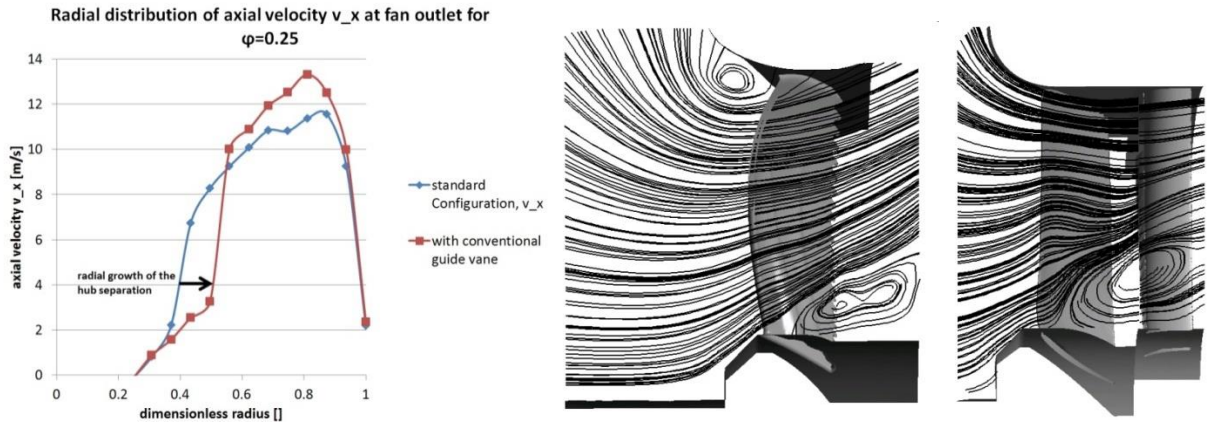

Figure 4: Axial velocity distributions downstream of the fan as function of the dimensionless radius, 5-hole-probe experiment (left), meridional streamlines from CFD simulations for the fan without guide vane (middle) and with conventional guide vane (right) at $\varphi = 0.25$

In *Figure 4*, results of the 5-hole-probe tests are presented comparing the experimental setups without and with conventional guide vane. The region of hub separation (defined here as the region with axial flow velocities lower than 4 m/s) is increased, at the same volume flow rate, by the application of the guide vane. Subsequently, the axial velocity components are higher in the non-detached region of the flow. This leads to higher dynamic losses concerning the axial velocity contribution and additionally to higher hydrodynamic losses. The energy flow chart for the conventional guide vane configuration (derived by use of a CFD simulation) is shown in *Figure 5*.

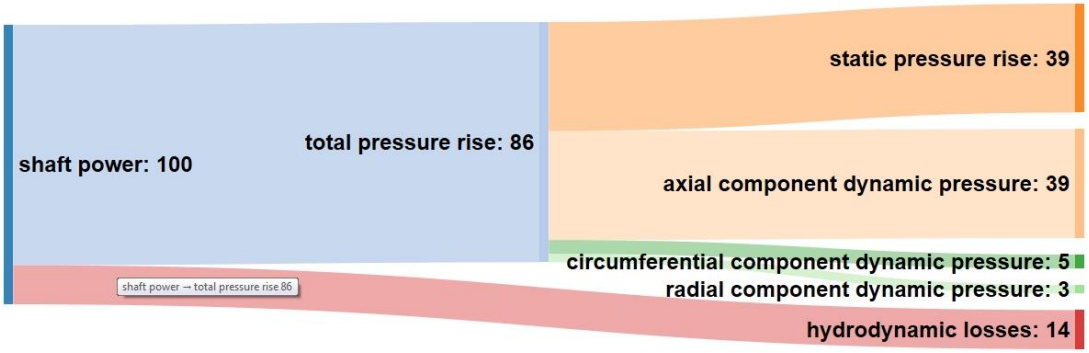

Figure 5: Partition of shaft power to different types of fluid energy for an axial fan with conventional guide vane at $\varphi = 0.25$ *and* $\psi_{stat} = 0.14$. *All numbers in %.*

Compared to the case without guide vane, *Figure 4*, the static efficiency is decreased by 3% points. The guide vane reduces the circumferential velocity, thus the dynamic pressure part by the circumferential velocity is significantly reduced. But rather than to react it to static pressure, it seems to be transformed to axial dynamic pressure, being in coherence with the 5-hole-probe results at the left of *Figure 4*. The hub separation region is increased, reducing, at the same volume flow rate, the effectively used area for the main flow A_{eff}. It seems that in cases with already present hub separation, conventional guide vane designs transform swirl velocity mainly to axial velocity rather than to static pressure, increasing therefore the hub separation region. Additionally, the hydrodynamic losses are increased mainly due to the presence of the guide vane itself with inherent friction and inertia losses. In *Figure 4*, CFD results for $\varphi = 0.25$ are printed in comparison between the case without guide vane (middle) and the case with conventional guide vane (right). In accordance to the 5-hole-probe measurements, the hub dead water region is increased when the conventional guide vane is present even though the flow is, for this case, better guided parallel to the axial direction at the longer shroud contour. This leads to higher axial velocities in the radially outer part of the air duct. The conventional guide vane design was taken as starting point for the optimization of a guide vane leading to higher static efficiencies of the fan.

CFD SIMULATIONS FOR FANS WITH LOW HUB-TO-TIP RATIO

Basis CFD model

For the reference CFD simulations (basis CFD model), a domain decomposition as presented in *Figure 6* has been used.

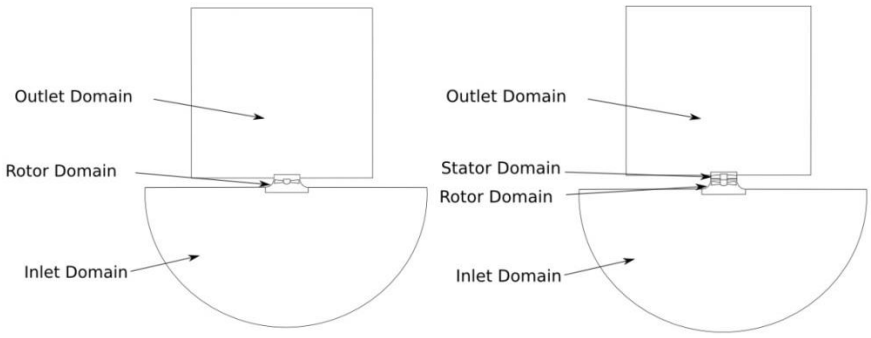

Figure 6: Simulation domains in the basis CFD model

The entire domain consists of several subdomains: The Inlet Domain (stationary), the Rotor Domain (rotating), the Stator Domain (stationary) in the case that a guide vane is present, and the Outlet Domain (stationary). This is a typically used configuration when simulating such a configuration. The numerical tool used within the present work is ANSYS CFX. The simulations were steady RANS simulations. Incompressible simulations have been carried out with air data. Only one blade passage was modelled both for rotor and stator, using periodical boundary conditions. At wall boundaries, prism layers were applied (using 9 prism layers), where a value of Y^+ in the range of 15-25 was realized. As turbulence model, the 2-equation SST-model, described in [11], was used, and wall functions have been applied. At the inlet, the mass flow and the turbulence intensity of 5% was prescribed. At the outlet, the average pressure was prescribed. Between Rotor Domain and Stator Domain, a mixing plane was applied. For the basis CFD model, about 500·000 unstructured elements for a simulation without guide vane and about 700·000 for a simulation with guide vane have been used. One simulation takes a wall time of about 2 hours using 32 cores in parallel.

Comparison of results using the basis CFD model simulation with experimental data

In *Figure 7*, where the efficiency is plotted as function of the dimensionless volume flow (left), both for a numerical simulation (basis CFD model) and an experimental measurement. Whereas the simulation results match the experiment well for high volume flow rates, an increasing divergence can be observed with decreasing volume flow rates. One explanation is the increased presence of unsteady flow regions within the simulation domain for higher throttled operating points.

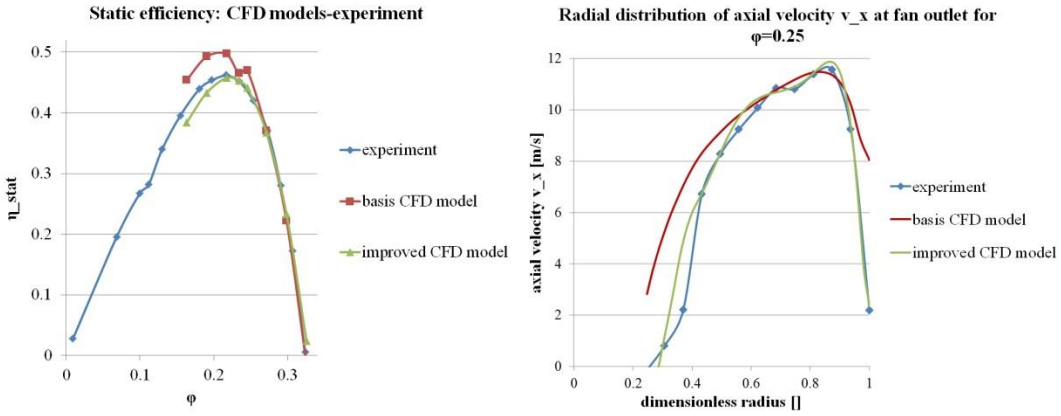

Figure 7: Comparisons of results of an experiment and CFD models (static efficiency over volume flow rate, left) and radial distribution of v_x (right)

We identified as an important reason the appearance of a hub separation region. Indeed, by comparison to 5-hole-probe experiments, we found that the separation line between main flow and hub wake was usually predicted at too small radii using the basis CFD model, underestimating the deficiency caused by it. Referring to *Figure 7* (left), hub dead water starts to occur in the CFD simulation (red line) at the first kink when moving from higher to lower volume rates at $\varphi = 0.23$. In the experiment, the occurrence of hub dead water has its onset already for higher volume flow rates at about $\varphi = 0.26$. In the right diagram of *Figure 7*, a comparison of the radial distributions of axial velocities between 5-hole-probe experiments and CFD simulations at $\varphi = 0.25$ and is presented. One clearly sees that hub dead water is much less pronounced for the basis CFD model (red line) compared to the experiment. This was an unsatisfactory result, as the optimization of a guide vane especially for the presence of hub dead water seemed not to be promising when based on CFD simulations which do not predict correctly the extent of the hub dead water region. One candidate method in order to improve the results may be seen in unsteady simulations. Applying unsteady simulation (Unsteady RANS), improvements could be observed, but the computational costs were too high in order to carry out an optimization process.

Improved CFD model

In further numerical experiments, techniques have been investigated to simulate fan configurations of interest without discretizing the outlet domain, as outlined in the sketches in *Figure 8*, predicting with good accuracy pressure rise and hub dead water extent even for highly throttled operating points.

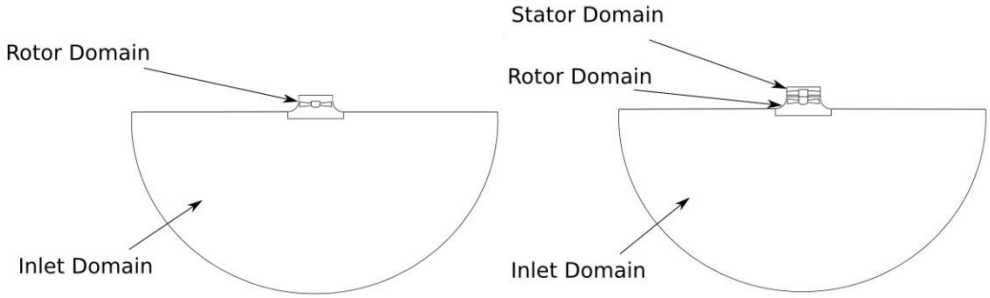

Figure 8: Simulation domains in improved CFD model

The crucial point is the boundary condition downstream of the fan rotor or the guide vane respectively. Just prescribing an average static pressure directly downstream of the fan leads to unsatisfactory results in terms of pressure rise characteristic and hub dead water extent, because this boundary condition has an unphysical effect on the upstream flow. In such cases, the application of a radial equilibrium boundary condition described for example in [12] is a promising approach. In a circumferentially averaged way, a static pressure *p* as function of the radius is prescribed at the outlet directly downstream the fan (rotor or stator, respectively). This distribution of *p* is calculated from the actual velocity field (namely from the distribution of the circumferential velocity component v_θ) of the simulation using the radial equilibrium correlation $\frac{\partial p}{\partial r} = \rho \cdot \frac{v_\theta^2}{r}$ and the ambient pressure at the outer radius. The radial equilibrium correlation, however, is only adequate if no meridional streamline curvature is present what is not guaranteed in the present configuration. So a modified radial equilibrium correlation of the form $\frac{\partial p}{\partial r} = C \rho \frac{v_\theta^2}{r}$ was used, where the free parameter C was calibrated with a number of simulations to match at best to some experimental data. We found the value of $C = 0.7$ to give satisfactory results both in terms of static efficiency prediction and the prediction of the hub dead water region. This kind of boundary condition does not affect the upstream flow in a critical way. Firstly, the radial distribution of the pressure field

prescribed is directly governed by the velocity field resulting from the upstream flow. Secondly, the circumferential distribution of the pressure field is free as the pressure field is only prescribed in a circumferentially averaged way. In the left graph of *Figure 9*, for a simulation using the proposed boundary condition, a distribution of the circumferential velocity v_θ is shown at the outlet of one blade passage, and on the right graph, the corresponding distribution of the pressure p imposed in circumferentially averaged way as boundary condition is shown for $\varphi = 0.25$. The hub dead water region is visible both regarding the boundary data and regarding the streamlines on the impeller blade.

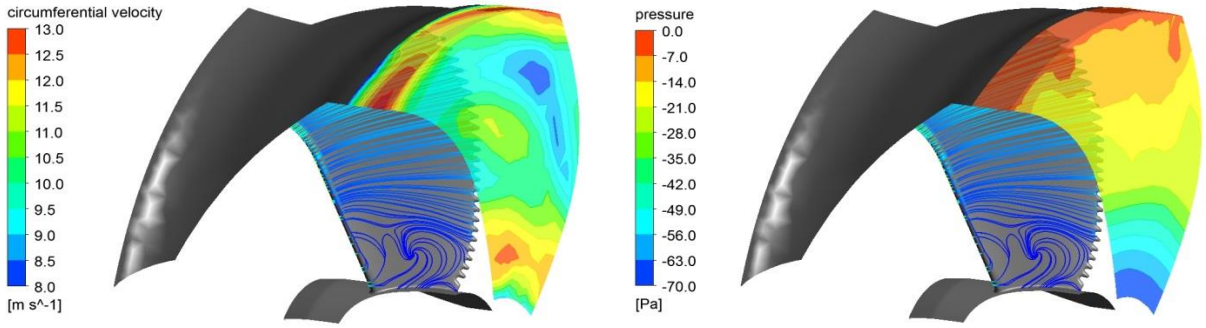

Figure 9: Distribution of v_θ at the outlet of one blade passage (left) and corresponding distribution of pressure (right) in a simulation with the improved CFD model for $\varphi = 0.25$

The graphs in *Figure 7*, considering the "improved CFD model", show the improvement achieved with this kind of boundary condition compared to the basis CFD model for the configuration without guide vane. The comparison of the static efficiency obtained from the numerical simulation compared and the experimental data (left diagram) is very good showing that the model is adequate for an optimization process considering the static efficiency. We note that the static pressure at the outlet for radially inward lying positions may take values below the ambient static pressure of the downstream environment. The static efficiency η_{stat}, however, is computed using the ambient static pressure. The explanation for that is that a part of the circumferential velocity component is reacted to static pressure in the not discretized space downstream the fan, as described by Laux [8], who gives as recovery factor for the swirl energy values of 62 % – 65 %. In all energy flow charts presented within this work, the recovered part of the swirl energy was already added to the static pressure branch. The significant recovering of static pressure from swirl energy even without guide vane is a further reason, why efficient guide vane design is in these cases a challenging. An important advantage of the improved CFD model is that the convergence time is comparatively low; using about 300·000 unstructured elements for a simulation without guide vane and about 500·000 for a simulation with guide vane, an operating point can be simulated in a simulation time of about 15-25 minutes using 32 cores in parallel. This allows an effective numerical optimization process.

OPTIMIZATION PROCESS FOR THE COMPACT GUIDE VANE UNIT BASED ON CFD SIMULATIONS

Parametrization of a guide vane unit

The parametrization of the guide vane unit is briefly described in this section. The parts of the unit being parametrized are the outer housing contour and the guide vane blades. The hub contour was fixed to the diameter of the impeller hub defined by the outer contour of the motor. The housing contour consists of an inlet nozzle constructed by two radii, a cylindrical part in the impeller region, and a conical diffuser, whose opening angle and onset axial position are free parameters. It was possible that the guide vanes blades lie axially within the diffusor part, enabling the possibility of

high axial packaging. Both the housing diameter in the cylindrical region and the hub diameter were fixed in accordance to the fixed impeller geometry. The axial extension of the unit was fixed as a constraint on axial compactness to 125 % of the axial extension of the configuration without guide vane corresponding to *Figure 1.* Axial compactness, however, turned out to be favorable for the guide vane design, similar to the results described in [5]. The construction principle of the guide vane blades used in the present work is it to define n_{sec} blade sections at different radii $R_i, i = 1 \ldots n_{\mathrm{sec}}$. The blade surfaces (suction side, pressure side, leading edge region and trailing edge region) are then built by construction of spline surfaces containing the curves of the different sections.

Definition of guide vane blade sections

The geometry of each section is built in two steps: First, a centerline is constructed, and second, a thickness distribution is superimposed in both directions perpendicular to the centerline. The centerline is parametrized by its axial and circumferential positions x_m and θ_m, its axial extension l, the leading edge angle β_{le}, the trailing edge angle β_{te} and the angle β_m at intermediate axial extension. The thickness distribution is not subject to the optimization. A thickness distribution is used having its maximum at 30 % axial chord length (NACA 4-digit without camber and modification to have finite trailing edge). The choice of the thickness is relying on stability and manufacturing issues.

"Semi-automatic" optimization loop for guide vane geometry based on CFD simulations

The guide vane geometry has been optimized based on CFD simulations relying on the improved CFD method. All simulations have been carried out using the same reference rotor geometry of diameter 630 mm with hub ratio $\nu = 0.24$. In order to evaluate one guide vane unit, four different operating points have been computed: an operating point near the stall point ($\varphi = 0.15$), the point near maximum static efficiency ($\varphi = 0.2$), an intermediate duty point ($\varphi = 0.25$) and one for high volume flow rate ($\varphi = 0.3$). The total efficiency $\eta_{tot,x}$ averaged over the three duty points was the major optimization target, which has at given volume flow rate φ the same behavior than the static efficiency η_{stat} and has the advantage not to approach to zero for high volume flow rates. If the fan configuration runs into stall at $\varphi = 0.15$, this gives a high penalization to this average total efficiency. The optimization has been carried out in a "semi-automatic" optimization process as lined out in the flow chart at the left of *Figure 10.* It can be seen that the entire process from the choice of a parameter set to the computation of the final results (i.e. the average total efficiency) is realized in a fully automatic way. This includes geometry construction, meshing, simulation setup, the simulation itself and post-processing. The only non-automatic action is the generation of new parameter sets based on previous simulation results. In the described way, over 150 guide vane unit geometries have been analyzed in order to find an optimum parameter set.

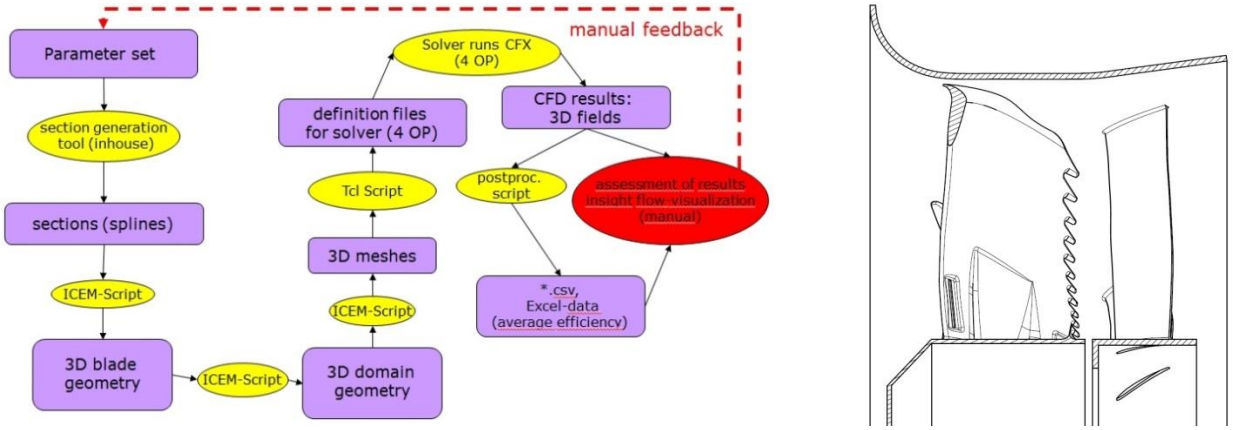

Figure 10: "Semi-automatic" optimization loop (left) and meridional cut of compact guide vane unit with fan (right)

RESULTS

Description of the aerodynamic parts of the optimized guide vane unit

In this section, the compact guide vane unit resulting from the optimization process and its properties are described. A meridional cut of the best analyzed guide vane unit is shown with a fan at the right of *Figure 10*. The housing contour contains the inlet region (left), a cylindrical part, where the rotor is positioned and a diverging, diffusor-like part (right). The opening angle of the diffusor is six degrees. The 11 guide vane blades are axially positioned within the diffuser region. The tip region of the guide vane blades lies axially slightly upstream compared to the root region. The hub diameter is identical to the rotor diameter. In Table 1, the axial extent l, the blade leading edge angle β_{le} and the blade trailing edge angle β_{te} angles are given at three sections. The blades are axially very compact. What is remarkable is the low difference of blade angle between leading edge and trailing edge. Especially at the hub, the trailing edge blade angle is high ($\beta_{te} = 43^{\circ}$), which is in contrast to conventional guide vane designs, where the trailing edge blade angle is in the region of zero or below in order to reduce the swirl component as much as possible. This trailing edge blade angle ensures that the ratio v_θ / v_x does not become too high (not higher than about 1) stabilizing the hub-near flow, without a too high flow deflection by the guide vane. So the guide vane has primarily the function of stabilizing the hub-near flow rather than transforming the circumferential velocity dynamic pressure to static pressure.

Table 1: Axial extension, leading edge and trailing edge angle of blade chord line against axis for three sections (diameter 630 mm)

	l	β_{le}	β_{te}
Section 1 (outer housing)	48 mm	35°	24°
Section 2 (midspan)	46 mm	33°	27°
Section 3 (hub)	49 mm	61°	43°

Aerodynamic and efficiency results

Experimental aerodynamic results are presented in *Figure 11*. In the left graph, the static pressure rise is plotted against the volume flow rate. Especially for lower volume flows, the pressure rise is significantly higher with the guide vane unit. The stall margin is enhanced by about 12 %. In the right graph, the static efficiency is plotted. The maximum static efficiency is augmented by use of the optimized guide vane unit to 59 % compared to 48 % for the fan without guide vane, meaning a gain of 11 % points, representing a relative increase of maximum static efficiency of about 23 %.

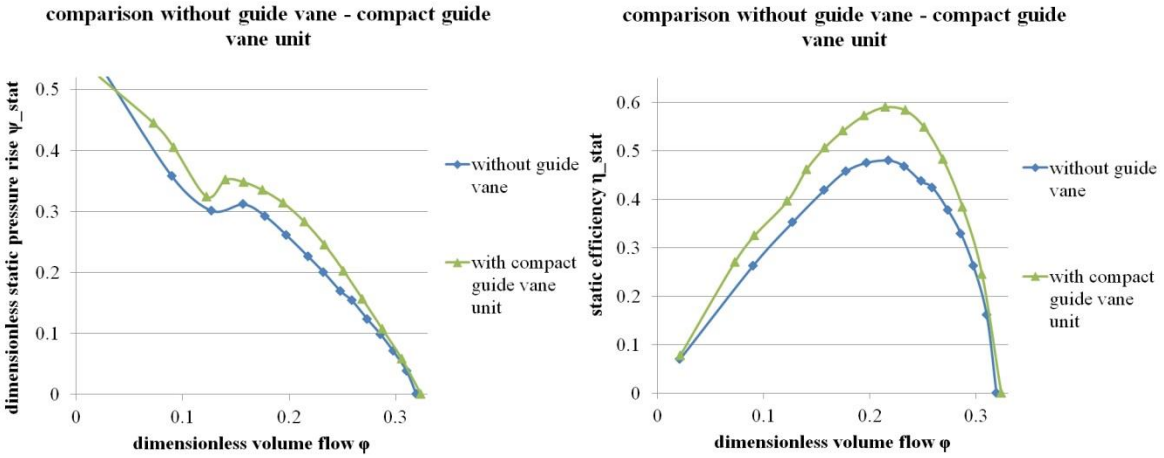

Figure 11: Comparison the case without guide vane to the optimized guide vane unit (experimental data).

In *Figure 12*, the partition of shaft power to the fluid is illustrated. The data was obtained by evaluation of a CFD simulation, and has been evaluated for the dimensionless volume flow rate $\varphi = 0.25$. Compared to the case without guide vane, both the dynamic pressure of the axial velocity component and the dynamic pressure of the circumferential velocity component have been significantly reduced. Concerning the circumferential component, we can see that the optimized guide vane unit reduces the swirl velocities, but the reduction is less than in the case of the conventional guide vane (*Figure 5*). The reason for that is the smaller flow deflection of the blades in circumferential direction. Concerning the axial component, the reduction comes, at the same volume flow rate, from the increase of the area A_{eff} being effectively available for the main flow. This comes from two mechanisms: the reduction of hub dead water and the diverging housing contour.

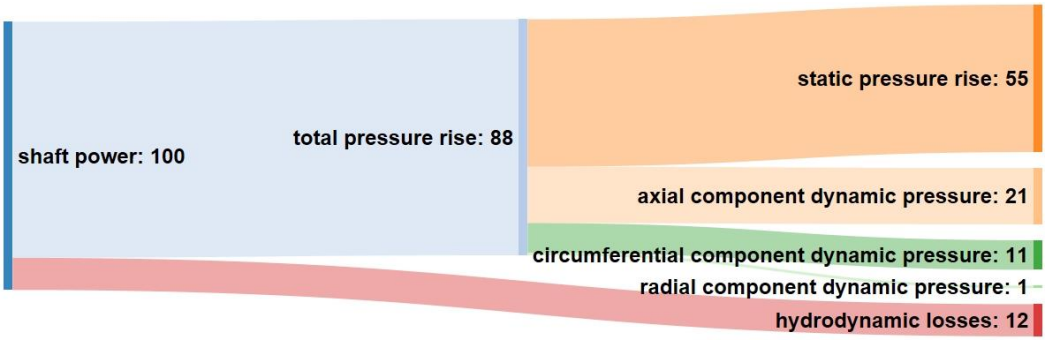

Figure 12: Partition of shaft power to different types of fluid energy for an axial fan with optimized guide vane unit at $\varphi = 0.25$ *and* $\psi_{stat} = 0.2$. *All numbers in %.*

The reduction of hub dead water can be observed in the comparison of CFD simulation results shown in *Figure 13*

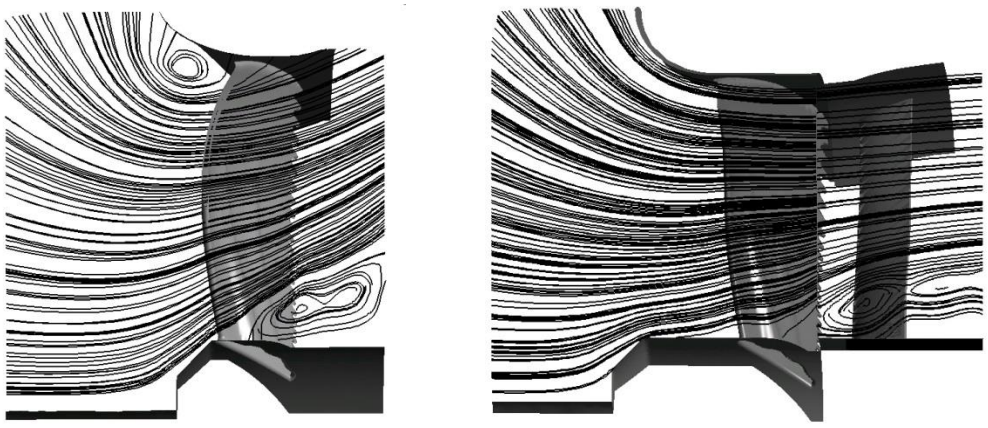

Figure 13: Comparison of meridional streamlines at the same volume flow rate for fan without guide vane (left) and fan in optimized guide vane unit (right)

CONCLUDING REMARKS

For low pressure fans with low hub-to-tip ratios $\nu = R_{Hub} / R_{Tip}$, the presence of a detached and highly recirculating flow region near the hub, called hub dead water, is an important limiting factor when designing highly efficient fans. Such fans are widely used without guide vanes, due to cost and compactness consideration, but also, because the design of efficient guide vanes is not well understood in the presence of significant hub dead water.

Classical guide vane design [7, 9] leads to the undesired effect that the region of the hub dead water increases, reducing the axial cross section area engaged by the main flow. Indeed, it was observed that such guide vane designs may just transform circumferential velocity components to axial velocity components, contracting the flow region in a meridional plane rather than transforming the dynamic energy to pressure. Thus, the separation surface between main flow and hub dead water is shifted radially outwards. As the presence of guide vane blades causes additional hydrodynamic losses, so designed guide vanes may even be detrimental to static efficiency.

Experimental results confirming the presence of a hub wake have been presented, both for configurations with and without guide vanes. For the development of an efficient guide vane design, we relied on CFD simulations. The simulation quality of axial fans at the presence of hub separation was investigated, and a method was worked out and calibrated to experimental data, which is based on a modified radial equilibrium correlation that allows it to simulate with good accuracy fan duty points with hub dead water being present, using a quite cost-efficient steady state RANS CFD simulation.

Result of a semi-automatic optimization, which has been carried out in order to develop an efficient guide vane unit, is a special guide vane design increasing by about 25% the static efficiency of axial fans with low hub-to-tip ratio. This compact unit, which can be manufactured as injection molded plastic piece, also incorporates the outer fan housing, motor support, and a short diffuser region. This concept makes the guide-vane technology very cost-effective, even for low-pressure axial fans under the constraint of high axial packaging.

VARIABLE SYMBOLS, DEFINITIONS, UNITS

D	$[m]$	inner diameter of the fan housing
$R = \frac{D}{2}$	$[m]$	inner radius of the housing, used as reference length
n	$\left[\frac{rev}{s}\right]$	rotation frequency of the impeller
ρ	$\left[\frac{kg}{m^3}\right]$	fluid density
$A_{ref} = \pi R^2$	$[m^2]$	reference area
$u_{ref} = 2\pi R \cdot n$	$\left[\frac{m}{s}\right]$	reference velocity
$\dot{V}$	$\left[\frac{m^3}{s}\right]$	volume flow
M	$[N \cdot m]$	shaft torque
$P_{shaft} = 2\pi M \cdot n$	$[W]$	shaft power
Δp_{stat}	$[Pa]$	static pressure rise of the fan
$\varphi = \frac{\dot{V}}{A_{ref} u_{ref}}$	[ ]	dimensionless volume flow
$\psi_{stat} = \frac{\Delta p_{stat}}{0.5 \cdot \rho \cdot u_{ref}^2}$	[ ]	dimensionless static pressure rise
$\lambda_{shaft} = \frac{P_{shaft}}{0.5 \cdot \rho \cdot A_{ref} u_{ref}^3}$	[ ]	dimensionless shaft power
$\eta_{stat} = \frac{\varphi \cdot \psi_{stat}}{\lambda_{shaft}}$	[ ]	static efficiency

BIBLIOGRAPHY

[1] Strscheletzky M.: *Gleichgewichtsformen der rotationssymmetrischen Strömungen mit konstantem Drall in geraden zylindrischen Hohlräumen.* Voith Forschung und Konstruktion, Book 5, Essay 1, **1959**

[2] Strscheletzky M.: *Zur Berechnung der Gleichgewichtsformen von rotationssymmetrischen Strömungen mit konstantem Drall in langen zylindrischen Hohlräumen.* Voith Forschung und Konstruktion, Book 8, Essay 7, **1962**

[3] Lindemann, T. B.: Optimale Niederdruckaxialventilatoren - *Optimale Niederdruck-Axialventilatoren für den Einsatz bei kleinen Reynoldszahlen.* Forschungsvereinigung Luft- und Trocknungstechnik e.V. (FLT), **2010**

[4] Lindemann, T. B.; Friedrichs; J., Stark, U.: *Development of a New Design Method for High Efficiency Swept Low Pressure Axial Fans With Small Hub/Tip Ratio.* In: ASME Turbo Expo 16-20. June **2014**

[5] Bakir, F.; Rey, R.; Moreau, S.: *Latest Developments in Automotive Engine Cooling Fan Systems Rotor-Stator Interactions.* Proceedings of the 3rd ASME, JSME Joint Fluids Engineering Conference, July 18-23, 1999, San Francisco, California, 4, pp. 487-496, American Society of Mechanical Engineers, **1999**

[6] Bakir, F.; Moreau, S.; Rey, R.; Henner, M; Borg, V.: *Experimental aeroacoustical analysis of efficient automotive engine cooling systems*. Proceedings of Fan 2012 Symposium, Senlis, **2012**

[7] Bohl, W.: *Technische Strömungslehre.* 12. edition, Vogel-Fachbuch, Würzburg, **2002**

[8] Laux, H.: *Beitrag zur experimentellen Untersuchung von Drallströmungen im kreiszylindrischen Rohr.* Dissertation, Berlin, **1961**

[9] Eck, B.: *Ventilatoren.* 6. Edition, Springer Verlag, **1991**

[10] Lewis, R.I.: *Turbomachinery Performance Analysis.* Book, Elsevier, **1996**

[11] Menter, F. R.: *Two-Equation Eddy-Viscosity Turbulence Models for Engineering Applications.* AIAA Journal, Vol. 32, No. 8 (1994), pp. 1598-1605, **1994**

[12] Koupper, C.; Poinsot, T.; Gicquel, L.Y.M; Duchaine, F.*: Compatibility of Characteristic Boundary Conditions with Radial Equilibrium in Turbomachinery Simulations.* AIAA Journal, American Institute of Aeronautics and Astronautics, vol. 52 (n° 12), pp. 2829-2839, **2014**